


 Cite this: *RSC Adv.*, 2021, **11**, 37952

## Physicochemical, morpho-structural, and biological characterization of polysaccharides from three *Polygonatum* spp<sup>†</sup>

 Jin-Bo Bai,<sup>‡,a</sup> Ji-Chun Ge,<sup>‡,b</sup> Wang-Juan Zhang,<sup>a</sup> Wang Liu,<sup>a</sup> Jian-Ping Luo,<sup>‡,b</sup> Feng-Qing Xu,<sup>acd</sup> De-Ling Wu<sup>\*acd</sup> and Song-Zi Xie<sup>‡,acd</sup>

*Polygonatum* species, including *P. cyrtonema*, *P. kingianum*, and *P. sibiricum*, are edible plants with medicinal purposes, which have long been consumed as food due to their high nutritional value. In this study, polysaccharides from *P. cyrtonema* (PCP), *P. kingianum* (PKP) and *P. sibiricum* (PSP) were obtained, and their physicochemical properties and *in vitro* biological activities were investigated. Our results demonstrated that PCP, PKP, and PSP consist of major fructose and minor glucose, galacturonic acid, and galactose in different molar ratios with the molecular weights of  $8.5 \times 10^3$  Da,  $8.7 \times 10^3$  Da, and  $1.0 \times 10^4$  Da, respectively. The three polysaccharides had triple-helical structures with  $\beta$ -D-Fruk,  $\alpha$ -D-Glcp,  $\alpha$ -D-Galp sugar residues, and an O-acetyl group, and displayed peak-shaped structures in different sizes. They also exhibited thermal, shear-thinning behavior and viscoelastic properties, and PCP presented the highest viscoelasticity. Moreover, they exerted strong free radical-scavenging abilities, and significant reducing capacity. PCP was the strongest, followed by PSP and then PKP. They significantly promoted the polarization of the M1 macrophage, with the effect of PCP ranking first. All three had similar effects on GLP-1 secretion. It is, therefore, necessary to identify the various roles of these three *Polygonatum* polysaccharides as functional agents based on their bioactivities and physicochemical properties.

Received 27th September 2021

Accepted 7th November 2021

DOI: 10.1039/d1ra07214e

[rsc.li/rsc-advances](http://rsc.li/rsc-advances)

## 1. Introduction

The rhizomes of *P. cyrtonema* Hua (PC), *P. sibiricum* F. Delaroche (PS) and *P. kingianum* Collett & Hemsl. (PK) belong to the Liliaceae family and have long been consumed in China. They are widely used to make tea, to cook meat, in soups, and during wine-making and are believed to be effective for invigorating Qi, promoting spleen and kidney health, and improving fatigue, anephithymia, diabetes, and lung problems.<sup>1,2</sup> There are several differences in the physiological and morphological characteristics of the three *Polygonatum* plants. However, it is unclear whether the rhizomes of *Polygonatum* have different chemical constituents and biological activities, which could lead to different uses.

Polysaccharides have been reported to be an important component of *Polygonatum* spp, and their levels indicate the quality of *Polygonatum*.<sup>2</sup> Polysaccharides with different chemical characteristics have been extracted from different *Polygonatum* species. It has been reported that glucofructans were obtained from PC,<sup>3,4</sup> glucomannans and galactomannan from PS,<sup>5,6</sup> and glucomannans from PK.<sup>7,8</sup> The various bioactivities of the three *Polygonatum* species, including immunomodulatory, anti-osteoporosis, neuroprotective, anti-oxidative, anti-fatigue, anti-aging, anti-tumor, and hypoglycemic activities, can be attributed to the different types of polysaccharides.<sup>2,4,9,10</sup> Although polysaccharides from PS, PC, and PK were analyzed based on saccharide mapping,<sup>2</sup> the majority of previous studies have focused on a single species. Therefore, a systematic comparison of the physicochemical characteristics and biological activities of the polysaccharides from three *Polygonatum* species needs to be determined under the same experimental conditions.

In our present work, the physicochemical properties including preliminary structural characterizations, tertiary structure, microstructure, thermal and rheological properties of the polysaccharides from PC, PS, and PK were investigated and compared using the same physical and chemical analysis methods. In addition, the *in vitro* antioxidant activity, the promotion of glucagon-like peptide-1 (GLP-1) secretion from

<sup>a</sup>School of Pharmacy, Anhui University of Chinese Medicine, Hefei, Anhui, 230012, China. E-mail: dlwu7375@ahcm.edu.cn; xiesongzi@ahcm.edu.cn

<sup>b</sup>School of Food and Biological Engineering, Hefei University of Technology, Hefei 230009, China

<sup>c</sup>Anhui Province Key Laboratory of Research & Development of Chinese Medicine, Hefei 230012, PR China

<sup>d</sup>Anhui Provincial Key Laboratory of New Manufacturing Technology for Traditional Chinese Medicine Decoction Pieces, Hefei 230012, PR China

<sup>†</sup> Electronic supplementary information (ESI) available. See DOI: 10.1039/d1ra07214e

<sup>‡</sup> These authors contributed equally to this work.



enteroendocrine L-cells, and the regulation of macrophage polarization of these polysaccharides were evaluated under the same bioactivity evaluation model.

## 2. Materials and methods

### 2.1 Materials and chemicals

The rhizomes of PC, PS, and PK (Fig. S1†) were respectively collected from Qinling mountain (Shaanxi Province, China), Jiuhua mountain (Anhui Province, China), and Ailao mountain (Yunnan Province, China), and were authenticated by Professor De-Ling Wu of Anhui University of Chinese Medicine. The voucher specimens were stored at the Chinese Materia Medica Resource Center of the Anhui University of Chinese Medicine. Dextrans with different molecular weights (5.0, 25.0, 80.0, 150.0, 420.0 and 670.0 kDa), monosaccharide standards including arabinose (Ara), glucose (Glc), fucose (Fuc), galactose (Gal), xylose (Xyl), mannose (Man), fructose (Fru), rhamnose (Rha), ribose (Rib), galacturonic acid (Gal-UA) and glucuronic acid (Glc-UA), and mannuronic acid (Man-UA), and dimethylsulfoxide (DMSO), 3-(4,5-dimethylthiazol-2-yl)-2,5-diphenyltetrazolium bromide (MTT), were obtained from Sigma-Aldrich Chemical Co. (St. Louis, MO, USA). Ferrozine, phenanthroline, phenazine methosulfate (PMS), 1,1-diphenyl-2-picrylhydrazyl (DPPH), 2,2'-azinobis(3-ethylbenzothiazoline-6-sulphonic acid) (ABTS), nitroblue tetrazolium (NBT), reduced nicotinamide adenine dinucleotide (NADH) were obtained from Aladdin Reagent Co. (Shanghai, China). The NO detection kit and RNAeasy<sup>TM</sup> Animal RNA Isolation kit were from Beyotime Biotechnology (Shanghai, China). ELISA kits for TNF- $\alpha$ , IL-12p70, IL-10, and TGF- $\beta$ 1 were from Solarbio Science & Technology Co. (Beijing, China). iScript<sup>TM</sup> cDNA Synthesis Kit and iTaq<sup>TM</sup> Universal SYBR Green Supermix were purchased from Bio-Rad Laboratories Inc. (Hercules, CA, USA). ELISA kit of GLP-1 was from Millipore (Billerica, MA, USA). FITC anti-mouse F4/80 and PE/Cyanine 7 anti-mouse CD86 antibodies were obtained from Biolegend (San Diego, CA, USA). APC anti-mouse CD206 antibody was from Invitrogen (Carlsbad, CA, USA). Other chemicals were of analytical grade and were obtained locally.

### 2.2 Preparation of polysaccharides

The fresh rhizomes of the three *Polygonatum* species were dried to a constant weight in an oven at 60 °C and were pulverized. The powder samples were soaked in 85% ethanol for 24 h with constant stirring at 37 °C and were filtered and centrifuged (3000g, 15 min) to obtain the residues after drying. The residues were extracted two times using distilled water (1 : 30, g : mL) at 80 °C for 2 h. After filtration, the supernatant was concentrated by a rotary evaporator under reduced pressure at 60 °C, and 100  $\mu$ L of  $\alpha$ -amylase (46 U mL<sup>-1</sup>) was added to the 600 mL of concentrated solution to hydrolyze starch at 60 °C for 1 h. The solution was then precipitated with a final concentration of 80% (v/v) ethanol for 24 h. After collection through centrifugation at 10 000g for 5 min, Sevag reagent was used to wipe out proteins from the precipitates, followed by dialysis (molecular weight

cutoff of 3500 Da) using distilled water for 48 h and lyophilization to obtain the refined polysaccharides.

### 2.3 Examination of general physicochemical properties

The anthrone-sulfuric acid method with glucose as a standard was employed to determine the total carbohydrate level.<sup>11</sup> Bradford's method with bovine serum albumin as a standard was used to detect the protein content.<sup>12</sup> The uronic acid content was determined using the *m*-hydroxybiphenyl method with Gal-UA as a standard.<sup>13</sup> Lignin, total polyphenols, total flavonoids, sulfate radical and ash contents were respectively examined by the reported methods as previously described.<sup>14</sup>

### 2.4 UV and FT-IR spectral analysis

The ultraviolet-visible spectra ranging from 190 to 400 nm of polysaccharide solutions were scanned using an ultraviolet spectrophotometer (Shimadzu 2550, Tokyo, Japan). After grinding with KBr powder, 2.0 mg of dried polysaccharide sample was analyzed using a Nicolet 6700 spectrometer in the range of 4000–400  $\text{cm}^{-1}$  to record FT-IR spectra (Thermo Nicolet, Madison, WI, USA).

### 2.5 Monosaccharide composition analysis

High-performance anion-exchange chromatography (HPAEC) was used to determine the monosaccharide composition of these polysaccharides. Briefly, 5 mg of polysaccharide sample was hydrolyzed with 1 mL of trifluoroacetic acid (TFA, 0.05 M) for 30 min at 100 °C in a sealed flask. The reaction mixture was dried by nitrogen gas and methanol was added to remove the excess acid. The hydrolysates (injection 20  $\mu$ L) were applied to an HPAEC-PAD system (Dionex ICS-5000, Thermo Fisher Scientific, USA) loaded with a CarboPac<sup>TM</sup> PA20 column (3 mm  $\times$  150 mm, Dionex, USA) at 30 °C. Double-distilled H<sub>2</sub>O (A) and 100 mM NaOH (B) were applied as the mobile phase with a flow rate of 0.5 mL min<sup>-1</sup>. Monosaccharides were identified according to the retention times of the standards (Fuc, Ara, Gal, Glc, Xyl, Man, Fru, Rib, Rha, Gal-UA, Glc-UA and Man-UA).

### 2.6 Molecular weight determination

The molecular weights of the prepared polysaccharides were analyzed using high-performance gel permeation chromatography (HPGPC) on an Agilent 1260 Infinity system equipped with a TSK G4000PWXL column (7.8 mm  $\times$  300 mm) connected to a TSK G5000PWXL column (7.8 mm  $\times$  300 mm). The polysaccharide sample (5 mg mL<sup>-1</sup>) was eluted with ultrapure water at 0.5 mL min<sup>-1</sup> and monitored with a refractive index detector (RID) at 30 °C. The molecular weights were measured using a standard curve that was established through different molecular weights of dextran standards.

### 2.7 Congo red test

In brief, 2.5 mg mL<sup>-1</sup> of polysaccharide solution was blended with 80  $\mu$ mol L<sup>-1</sup> of Congo red solution. Thereafter, the different volumes (0–4 mL) of NaOH solution (1 M) were slowly added to the mixture at final concentrations of 0, 0.05, 0.1, 0.15,



Table 1 Primer sequences of RT-PCR analysis

Genes	Forward primer	Reverse primer
IL-1 $\beta$	TTCAGGCAGGCAGTATCACTC	GAAGGTCCACGGGAAAGACAC
IL-12p70	CGCAGCTCTAGGAGCATGTG	AGTCCCTTGGTCCAGTGTG
TNF- $\alpha$	CCCTCACACTCAGATCATCTCT	GCTACGACGTGGGCTACAG
Arg-1	TTCTAAAAGGACAGCCTCG	CAGACCGTGGGTTCTCACA
IL-10	GCTCTTACTGACTGGCATGAG	CGCAGCTGTAGGAGCATGTG
TGF- $\beta$	TGGAGCAACATGTGGAACTC	TGCCGTACAACCTCCAGTGC
GADPH	AGGTCGGTGTGAACGGATTG	GGGGTCGTTGATGGCAACA

0.2, 0.25, 0.3, 0.35, 0.4, 0.45 and 0.5 mol L<sup>-1</sup>, respectively. A blank control was set using the mixed solution without polysaccharides. After balancing at room temperature for 10 min, the maximum absorption wavelength ( $\lambda_{\text{max}}$ ) was recorded from 200 to 600 nm using the ultraviolet spectrophotometer.

## 2.8 NMR analysis

The polysaccharide sample (90 mg) was exchanged sufficiently with deuterium oxide (D<sub>2</sub>O) by repeated lyophilization, and dissolved with D<sub>2</sub>O in a nuclear magnetic tube. The <sup>1</sup>H and <sup>13</sup>C NMR spectra were recorded on a Bruker Avance AV400 NMR spectrometer (Bruker, Switzerland).

## 2.9 Thermal analysis

The thermal gravimetric analysis (TGA) of the polysaccharide samples was operated on a Q600 thermogravimetric analyzer (TA Instruments, USA), warmed at 10 °C min<sup>-1</sup> from 25 to 800 °C, with nitrogen as the carrier gas.

## 2.10 Scanning electron microscopy (SEM)

The polysaccharides were sputtered with a gold layer *via* an ion sputter coater under reduced pressure. The images were recorded by a SEM system (Quanta FEG 250, FEI, USA) under high vacuum conditions at an acceleration voltage of 20 kV and image magnifications of 1000 and 10 000 times.

## 2.11 Atomic force microscopy (AFM) analysis

The polysaccharide solution at 10 µg mL<sup>-1</sup> (5 µL) was placed on freshly cleaved mica surfaces and air-dried for 4 h. The molecular morphological structures of the polysaccharides were analyzed by an AFM system (Bruker SCANASYST-AIR).

## 2.12 Rheological analysis

A Discovery HR-1 hybrid rheometer (TA Instruments, New Castle, USA) equipped with a cone-plate (60 mm diameter, 1 mm gap, 1° angle) was used to detect the rheological properties of polysaccharides at 25.0 ± 0.1 °C. Briefly, 8.0 mg mL<sup>-1</sup> of polysaccharide solution (7.0 mL) was transferred to the plate and balanced for 10 min before measurement. The apparent viscosity was detected at a shear rate range of 0.01 to 1000 s<sup>-1</sup>. Within the linear viscoelastic region, the storage modulus (G') and loss modulus (G'') were examined with a frequency sweep (0.01 to 100 Hz) at a 2% oscillation strain.

## 2.13 *In vitro* antioxidant activity assays

According to the reported methods,<sup>9,14</sup> to evaluate the antioxidant activities of the polysaccharides *in vitro*, the scavenging activities of DPPH, hydroxyl, ABTS and superoxide anion radicals, and the reducing power and ferrous ion-chelating capacity assays were performed. During the experiments, the different concentrations of polysaccharides solutions were set at 0.1, 0.2, 0.4, 0.6, 0.8, 1, 2, 3, 4, and 5 mg mL<sup>-1</sup>. The same concentration range of vitamin C (Vc) was used as the positive control for the DPPH, hydroxyl, ABTS, and superoxide anion radical scavenging, and the reducing power assays. In the ferrous ion-chelating capacity assay, EDTA-2Na was set as the positive control.

## 2.14 *In vitro* evaluation of GLP-1 secretion from the polysaccharide-stimulated NCI-H716 cells

NCI-H716 cells were obtained from the Cell Bank of Type Culture Collection of the Chinese Academy of Sciences (Shanghai, China) and were maintained with RPMI 1640 medium, 10% FBS and 1% penicillin/streptomycin. As described previously,<sup>10</sup> the cells (1 × 10<sup>6</sup> cells per mL) were seeded in a 48-well plate coated with Matrigel for 48 h and were respectively incubated with polysaccharide samples at 25, 50, and 100 µg mL<sup>-1</sup> for 2 h, and 50 µg mL<sup>-1</sup> PMSF was added. The

Table 2 Chemical properties and monosaccharide compositions of PKP, PCP, PSP<sup>a</sup>

Item	PKP	PCP	PSP
Yield (%), w/w)	9.65 ± 0.04 <sup>c</sup>	11.09 ± 0.24 <sup>b</sup>	15.43 ± 0.11 <sup>a</sup>
Carbohydrate (%)	97.54 ± 3.56 <sup>a</sup>	96.38 ± 1.78 <sup>a</sup>	95.86 ± 1.69 <sup>a</sup>
Protein (%)	0.25 ± 0.01 <sup>a</sup>	0.36 ± 0.02 <sup>a</sup>	0.24 ± 0.03 <sup>a</sup>
Uronic acid (%)	5.92 ± 0.93 <sup>b</sup>	3.33 ± 0.1 <sup>c</sup>	10.21 ± 0.71 <sup>a</sup>
Ash	N.D.	N.D.	N.D.
Lignin	N.D.	N.D.	N.D.
Total polyphenols	N.D.	N.D.	N.D.
Total flavonoids	N.D.	N.D.	N.D.
Sulfate radical	N.D.	N.D.	N.D.

### Monosaccharide composition (%)

Galactose	14.55 ± 1.25 <sup>a</sup>	2.32 ± 0.34 <sup>c</sup>	10.98 ± 2.02 <sup>b</sup>
Glucose	3.47 ± 0.02 <sup>b</sup>	3.27 ± 0.17 <sup>b</sup>	9.38 ± 0.76 <sup>a</sup>
Fructose	74.74 ± 3.65 <sup>b</sup>	92.44 ± 5.72 <sup>a</sup>	68.92 ± 2.87 <sup>b</sup>
Galacturonic acid	7.24 ± 0.17 <sup>b</sup>	1.97 ± 0.05 <sup>c</sup>	10.72 ± 0.54 <sup>a</sup>

<sup>a</sup> Results are expressed as mean ± SD. Different letters mean significantly different (*p* < 0.05) for the same item.



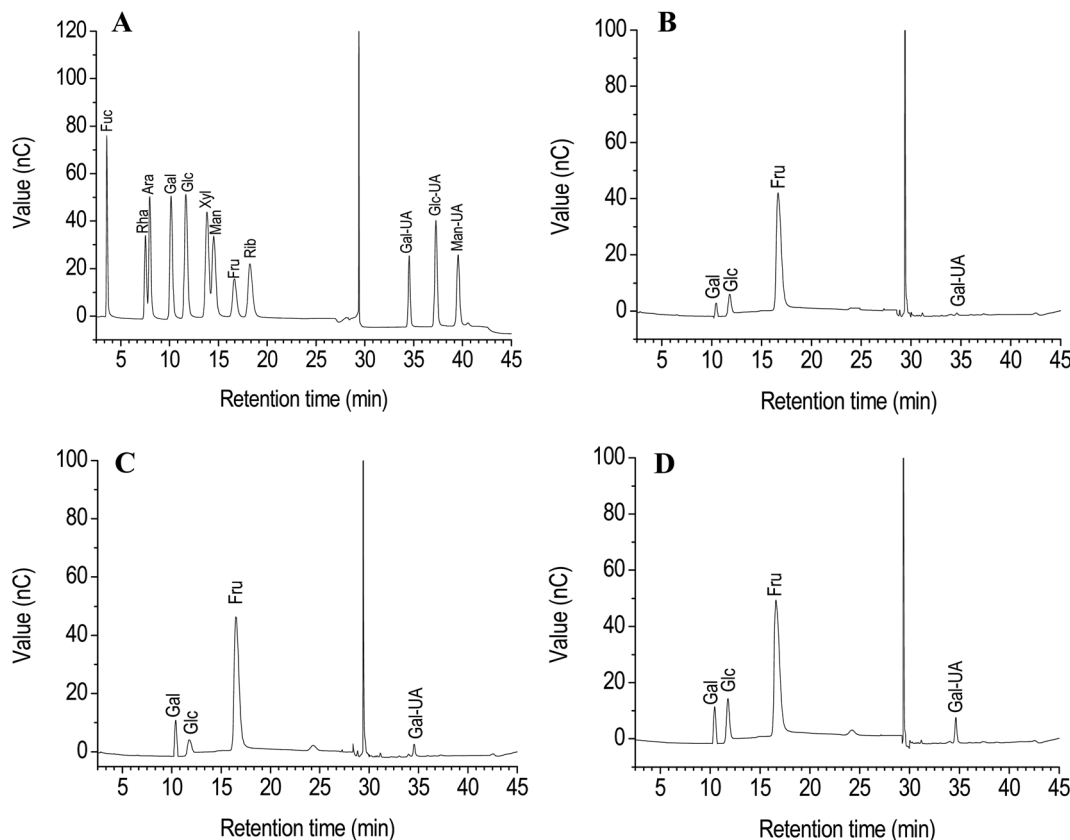


Fig. 1 HPAEC-PAD chromatograms of standard monosaccharides (A) and component monosaccharides of PCP (B), PKP (C), and PSP (D).

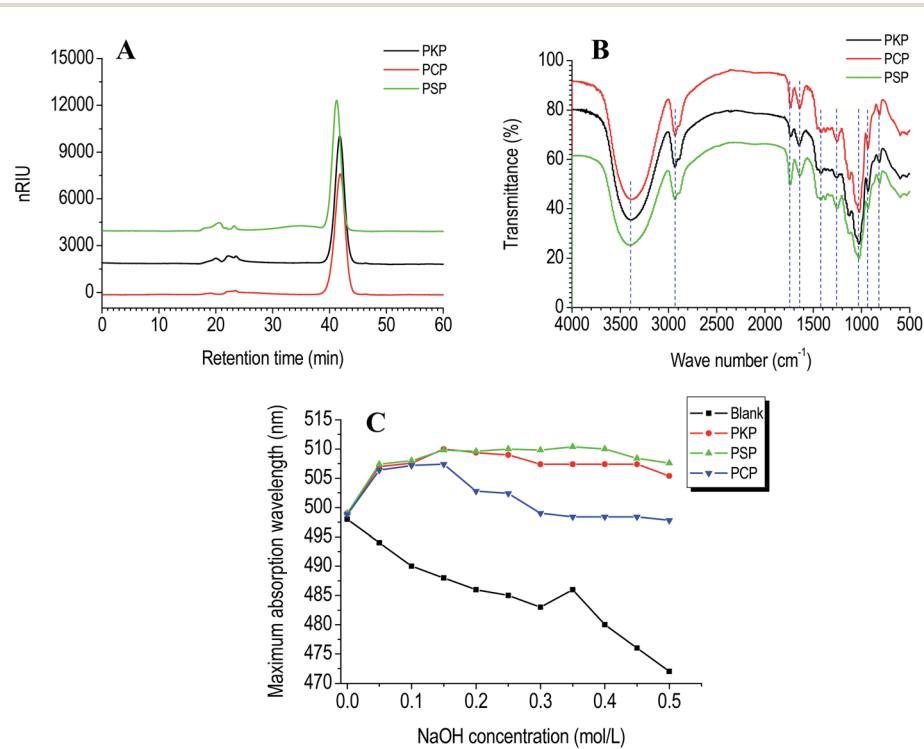


Fig. 2 HPGC chromatograms (A), FT-IR spectral (B), and triple-helical conformation analysis (C) of PCP, PKP, and PSP.



cells incubated in the medium without polysaccharides were used as the negative control. After centrifugation at 1000g (4 °C) for 15 min, the culture supernatant was gathered to detect the GLP-1 level using an ELISA kit.

## 2.15 *In vitro* assessment of polysaccharides on macrophages

**2.15.1 Cell culture.** DMEM medium containing 10% FBS and 1% penicillin/streptomycin was used to culture the RAW264.7 macrophages. The cells were cultured in a humidified incubator at 37 °C under humidified air with 5% CO<sub>2</sub>.

**2.15.2 Cell viability assay.** The effects of PCP, PKP, and PSP on the viability of RAW264.7 were measured using the MTT method.<sup>15</sup> RAW264.7 cells with a density of  $2 \times 10^5$  cells per mL were precultured in a 96-well plate for 24 h and then incubated with polysaccharides samples at different final concentrations (800, 400, 200, 100, 50, and 25  $\mu\text{g mL}^{-1}$ ) for another 24 h at 37 °C. After that, 20  $\mu\text{L}$  of MTT (5  $\text{mg mL}^{-1}$ ) was added to each well and incubated for 4 h in the dark at 37 °C. Finally, DMSO (200  $\mu\text{L}$ ) was added to stop the reaction and dissolve the

produced formazan crystals. DMEM medium was set as the control. The absorbance at 570 nm was detected.

### 2.15.3 Determination of nitric oxide (NO) and cytokines.

RAW264.7 cells at  $2 \times 10^5$  cells per mL were seeded in a 96-well plate for 24 h and were severally stimulated with PCP, PKP, and PSP at a final concentration range of 25 to 800  $\mu\text{g mL}^{-1}$  for 24 h. The culture supernatant was then harvested for the analysis of NO, IL-10, TNF- $\alpha$ , IL-12p70, and TGF- $\beta$  levels by ELISA kits with the manufacturer's instructions.

### 2.15.4 Quantitative RT-PCR analysis.

RAW264.7 cells at a density of  $5 \times 10^6$  cells per mL were cultured in a 24-well plate for 24 h and were then incubated with PCP, PKP, or PSP at 400, 200, and 100  $\mu\text{g mL}^{-1}$ . After 24 h of incubation, cells were collected by centrifugation ( $1000 \times g$  at 4 °C for 5 min) and washed three times with PBS. The total RNA was isolated using the RNAeasy™ Animal RNA Isolation Kit with Spin Column and was reverse-transcribed by the iScript™ cDNA Synthesis Kit in line with the manufacturer's instructions. For quantitative PCR, the reaction mixture containing 10  $\mu\text{L}$  2 $\times$  iTaq™ Universal SYBR® Green supermix, 1  $\mu\text{L}$  cDNA, 0.4  $\mu\text{L}$  of forward and

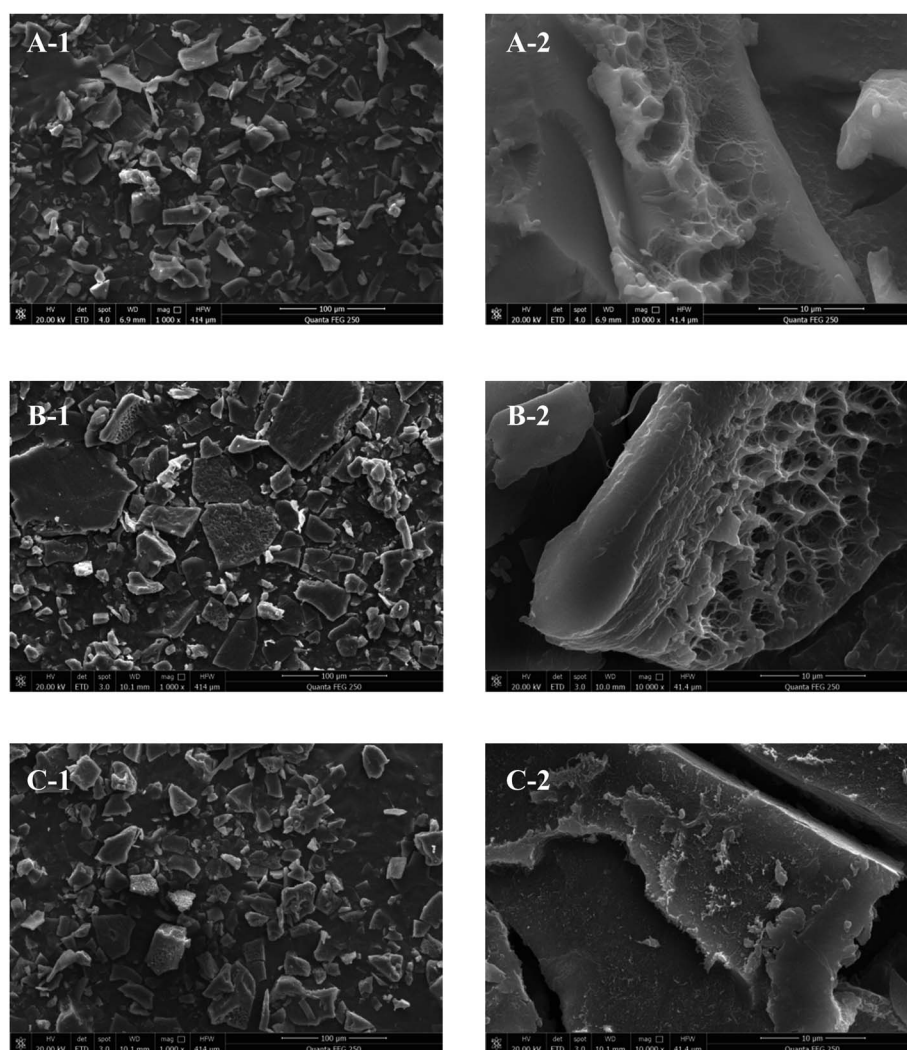


Fig. 3 Scanning electron micrographs of PKP (A), PCP (B), and PSP (C). (A-1–C-1)  $\times 1000$ ; (A-2–C-2)  $\times 10\,000$ .



reverse primers (IL-1 $\beta$ , IL-12, TNF- $\alpha$ , Arg-1, IL-10, and TGF- $\beta$ ), and 8.2  $\mu$ L of sterile water (PCR grade) was employed. The amplification program included pre-degeneration at 95 °C for 1 min, followed by 35 cycles of denaturation at 95 °C for 15 s, annealing, and elongation at 60 °C for 60 s. GAPDH was used as an internal control to normalize gene expression. The specific primers' sequences are shown in Table 1.

**2.15.5 Flow cytometry.** RAW264.7 cells ( $5 \times 10^6$  cells per mL) were seeded on a 24-well plate for 24 h and then treated with PCP, PKP, or PSP in increasing concentrations (100, 200, and 400  $\mu$ g mL $^{-1}$ ). After 24 h, the cells were digested, washed with PBS two times, and collected after centrifugation (1000  $\times g$ , 5 min). The single-cell suspensions ( $2 \times 10^5$  cells) were stained with FITC anti-mouse F4/80, APC anti-mouse CD206, and PE/Cyanine 7 anti-mouse CD86 antibodies for 30 min at

4 °C to analyze the phenotype of macrophages using a BD FACScan flow cytometer.

## 2.16 Statistical analysis

Statistical tests were analyzed by one-way analysis of variance (ANOVA) of SPSS software. Data were described as the mean  $\pm$  SD. The statistical differences between the groups were analyzed through Duncan's multiple-range test. Significant difference was statistically set as  $p < 0.05$  or  $p < 0.01$ .

## 3. Results

### 3.1 Characterization of the physicochemical properties of PCP, PKP, and PSP

**3.1.1 Yield and chemical analysis.** As shown in Table 2, the yields of polysaccharides from three *Polygonatum* spp were

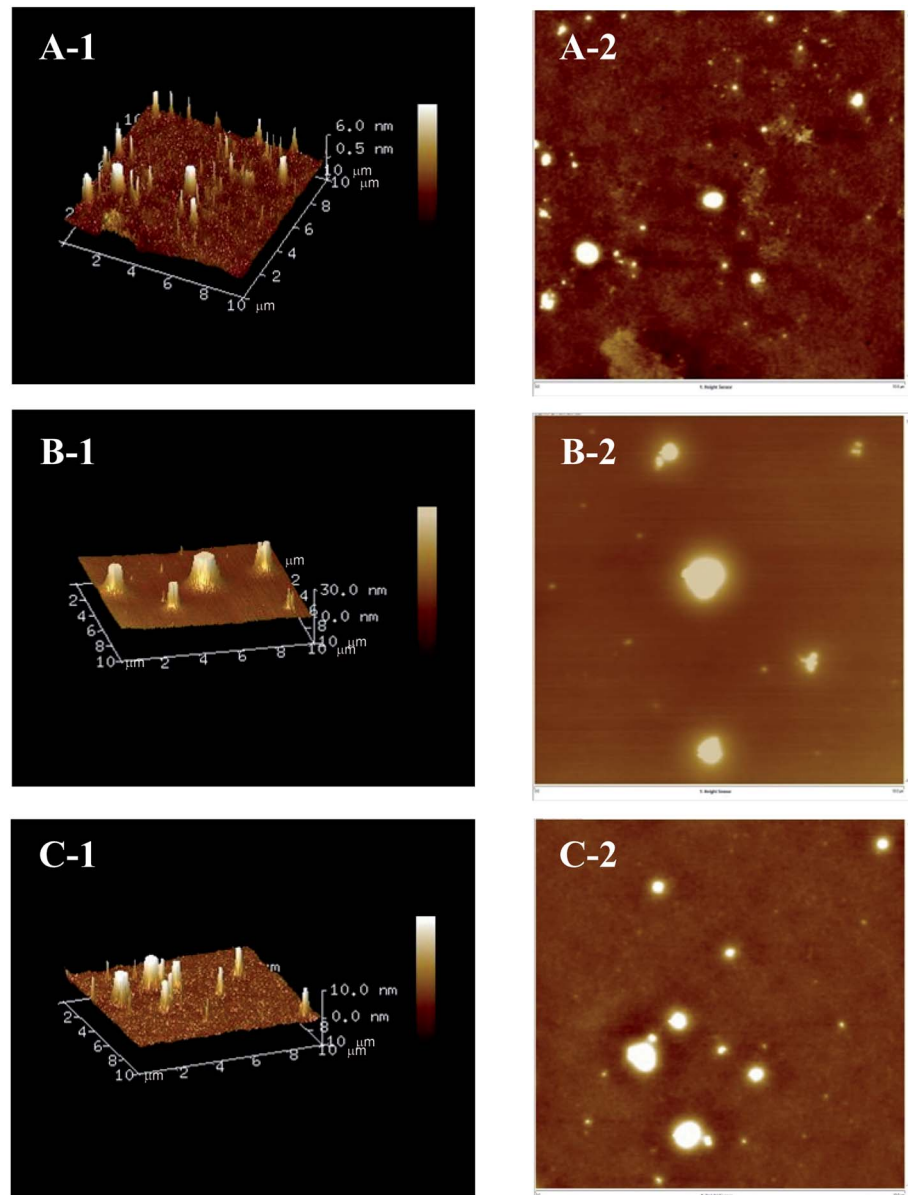


Fig. 4 Three-dimensional (A-1–C-1) and two-dimensional (A-2–C-2) AFM topographic images of PKP (A), PCP (B), and PSP (C).



11.09% for PCP, 9.65% for PKP, and 15.43% for PSP. The total carbohydrate contents of the three polysaccharide samples exceeded 90%. The protein content in each polysaccharide sample was less than 1%. The three polysaccharide samples all contained uronic acid and the amount of uronic acid was higher in PSP than in the other polysaccharides, which could be due to the differences in the growing conditions for the different *Polygonatum* species. The UV spectrum (Fig. S2†) indicated that PCP, PKP, and PSP had no absorption at 260 nm and almost no absorption peak at 280 nm. This indicates an absence of nucleic acid and the presence of little protein.

It has been demonstrated that strong acid hydrolysis can induce the transformation of fructose into mannose and glucose.<sup>16</sup> Therefore, dilute acid hydrolysis using the HPAEC-PAD method was performed to analyze the monosaccharide composition of PCP, PKP and PSP. The most fructose was found among the monosaccharides in the polysaccharides of *Polygonatum* species (Fig. 1). The fructose content of PCP exceeded 90% (Fig. 1A), while the fructose content in PKP and PSP was less than 80%. The glucose, galacturonic acid, and galactose were also observed in the PCP, PKP, and PSP (Fig. 1B–D). A higher galactose level was detected in PKP than the other polysaccharides (Fig. 1C). In addition, PSP had more galacturonic acid and glucose than PCP or PKP (Fig. 1D).

### 3.1.2 Preliminary structural characterization

**Molecular weight analysis.** The molecular weight of polysaccharides was measured by HPGPC with RID. It displayed that PCP, PKP, and PSP presented one primary symmetrical elution peak with respective  $M_w$  values of  $8.5 \times 10^3$  Da,  $8.7 \times 10^3$  Da, and  $1.0 \times 10^4$  Da (Fig. 2A).

**FT-IR analysis.** The functional group of polysaccharides was characterized by FT-IR spectroscopy. As presented in Fig. 2B, the FT-IR spectra of PCP, PKP and PSP were similar. Three samples had classical polysaccharide absorption peaks between 500–4000 cm<sup>−1</sup>. The strong peak at near 3500 cm<sup>−1</sup> revealed the O–H stretching vibration. The relatively weak peaks at around 2900, and 1000 cm<sup>−1</sup> indicated the characteristic stretching vibration of C–H and C–O, respectively. The absorption peak at around 1730 cm<sup>−1</sup> was assigned to the C=O vibration of esterified carboxylic groups (COO–R), while the peak at around 1600 cm<sup>−1</sup> was caused by the asymmetric stretching vibration of C=O in the carboxylate anions (COO<sup>−</sup>).<sup>17,18</sup> The vibration of C–O in O-acetyl groups was observed by the peak at 1260 cm<sup>−1</sup>.<sup>2,4,19</sup> Moreover, the absorption bands at 930 cm<sup>−1</sup> demonstrated that the PCP, PKP, and PSP all contained β-D-fructofuranose (Fruf).<sup>2,4,10</sup> The bands in the fingerprint region below 900 cm<sup>−1</sup> were due to the skeletal vibration of the pyranose ring.<sup>20</sup>

**NMR analysis.** <sup>1</sup>H and <sup>13</sup>C NMR spectra showed that PCP, PKP, and PSP all had the typical distribution of NMR signals ( $\delta_H$  3.0–5.3 and  $\delta_C$  60–110) of the polysaccharides.<sup>21,22</sup> In the <sup>1</sup>H NMR spectra of PCP, PKP, and PSP (Fig. S3A–C†), the signals at  $\delta$  4.00–4.15 ppm and  $\delta$  4.15–4.20 ppm were respectively assigned to H-4 and H-3 of D-Fruf residues.  $\delta$  3.60–3.85 ppm was attributed to H-1, H-5 and H-6 of D-Fruf residues, or H-2, H-3, H-4, H-5 and H-6 of D-GlcP.  $\delta$  5.33, 5.34 and 5.32 ppm were designated to H-1 of α-D-GlcP. In the <sup>13</sup>C NMR spectra, the small signals at  $\delta$  91.97 for PCP,  $\delta$  92.10 for PKP, and  $\delta$  93.10 for PSP were

assigned to C-1 of an internal α-D-glucopyranose (GlcP).<sup>3,4</sup> The anomeric signals of <sup>13</sup>C NMR at  $\delta$  62.22–63.39 ppm,  $\delta$  63.95–69.47 ppm,  $\delta$  75.33–76.59 ppm,  $\delta$  79.20–80.49 ppm,  $\delta$  81.11–83.35 ppm and  $\delta$  103.11–104.01 ppm were respectively attributed to C-1, C-6, C-4, C-3, C-5 and C-2 of β-D-Fruf residues (Fig. S2D–F†).<sup>4,10</sup> The anomeric carbon signals at  $\delta$  103.11,  $\delta$  103.64,  $\delta$  103.76, and  $\delta$  104.01 ppm were assigned to C-2 of →1)-β-D-Fruf-(2→, β-D-Fruf-(2→, →1,6)-β-D-Fruf-(2→, and →6)-β-D-Fruf-(2→, respectively, according to the previously reported studies.<sup>4,10</sup> In addition, the proton signals at  $\delta$  2.07 for PCP and  $\delta$  2.08 for PKP and PSP, the anomeric carbon signals at  $\delta$  174.21 and  $\delta$  20.15 for PCP,  $\delta$  173.97 and  $\delta$  20.15 for PKP,  $\delta$  173.97 and  $\delta$  20.35 for PSP confirmed presence of the O-acetyl group in the three *Polygonatum* polysaccharides.<sup>3,4,10</sup> This was consistent with the results from the FT-IR spectra. The distinct anomeric carbon signal at  $\delta$  98.08 ppm was observed in the <sup>13</sup>C NMR of PKP and PSP, though a small signal was observed in PCP. The signal at  $\delta$  98.08 ppm could be attributed to the C-1 of α-D-Galp or α-D-GalpA,<sup>4,22</sup> indicating that the content of Galp or GalpA was lower in PCP than in PKP or PSP. This further confirmed the results of our monosaccharide composition analysis.

**Tertiary structure.** Biopolymer conformations can affect their bioactivities.<sup>23</sup> When used as an acid dye, Congo red can combine with polysaccharides to form a helical conformation.<sup>24</sup> If polysaccharides have a triple-helix conformation, the

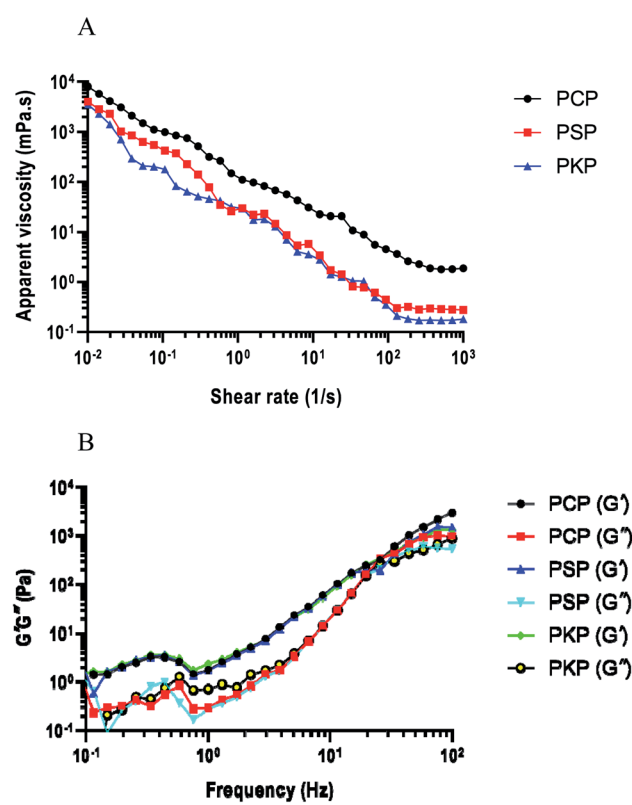


Fig. 5 (A) Viscosity–shear rate profiles of PCP, PSP, and PKP. (B) Storage modulus ( $G'$ ) and loss modulus ( $G''$ ) of three polysaccharides.



polysaccharide-Congo red complexes will lead to a red migration in the maximum absorption wavelength ( $\lambda_{\text{max}}$ ) compared to the Congo red control.<sup>14,25</sup> When treated with alkaline at high concentration, the helical conformation of biopolymers will be destroyed and  $\lambda_{\text{max}}$  will decrease.<sup>14</sup> Compared to the Congo red blank, an obvious red shift in  $\lambda_{\text{max}}$  of PKP, PSP or PCP-Congo red complexes was found at NaOH concentrations ranging from 0 to 0.15 mol L<sup>-1</sup> (Fig. 2C). This indicates that three *Polygonatum* polysaccharides all presented triple-helical conformations at low alkaline concentrations.

*The morphologies of the polysaccharides.* SEM is typically used to observe the surface morphologies of polysaccharides, which impact the properties of polysaccharides during their application.<sup>15,25</sup> As shown in Fig. 3, the surfaces of PKP, PCP, and PSP all displayed blocky structures in different sizes with relatively compact and smooth surfaces. PKP and PSP particles were smaller in size and had a more uniform size distribution than PCP, which exhibited irregular shapes with a larger, looser, and more porous surface area, indicating it has hydration properties.

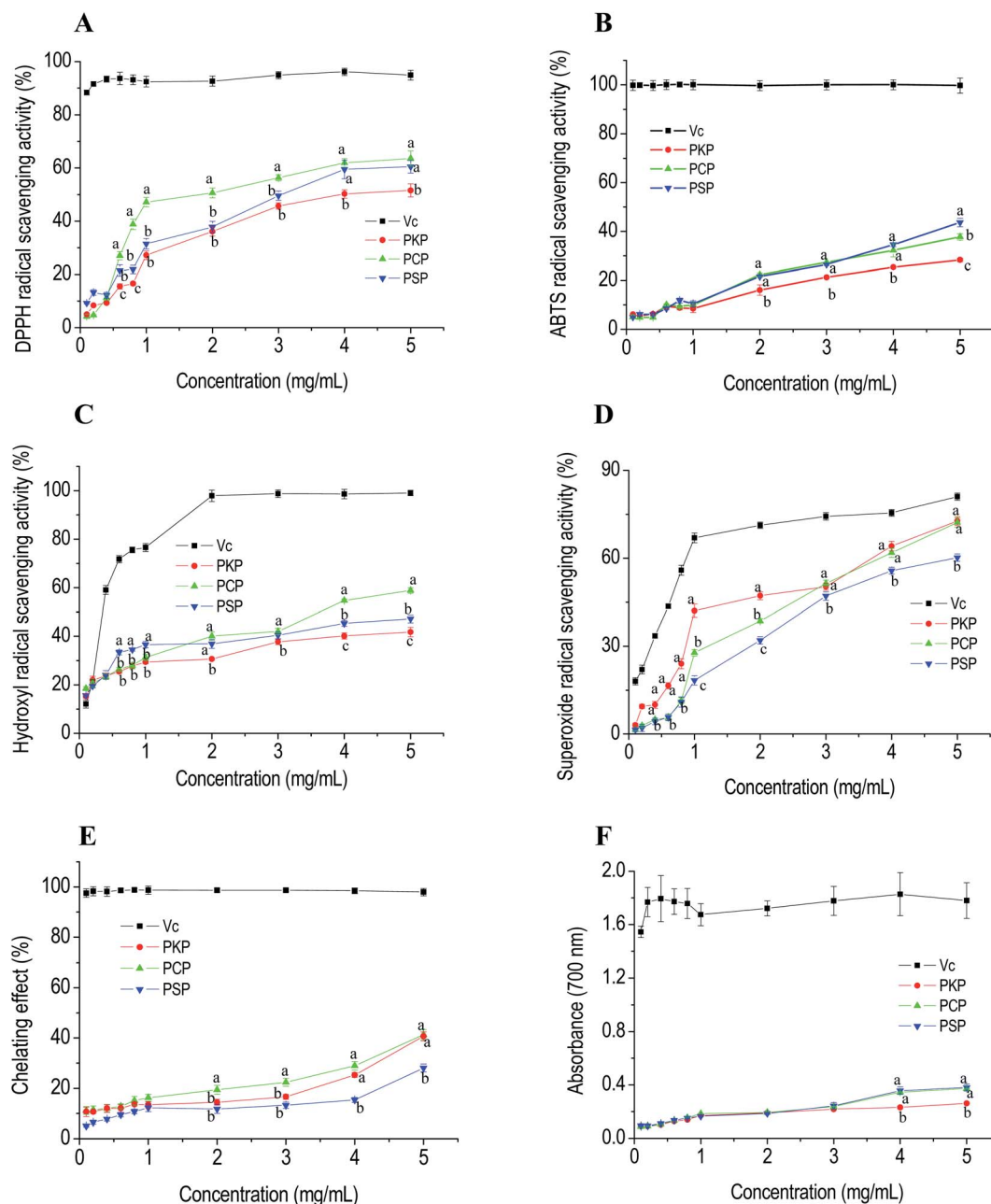


Fig. 6 *In vitro* antioxidant activities of PCP, PKP, and PSP evaluated by the DPPH (A), ABTS (B), hydroxyl (C), and superoxide (D) radical-scavenging abilities, and chelating capabilities (E), and the reducing power (F). Each value is expressed as the mean  $\pm$  SD (n = 3). Different letters indicate significant differences ( $p < 0.05$ ) between PKP, PCP, and PSP at the same concentration.

AFM is a powerful technology that can be used to directly observe the three-dimensional structural characteristics and molecular features of polysaccharides.<sup>26</sup> As presented in Fig. 4, the two-dimensional and three-dimensional AFM topographic images demonstrated that the three *Polygonatum* polysaccharides all had a peak-shaped structure, which could be caused by the highly intertwined sugar chains and numerous hydroxyl groups in polysaccharides.<sup>27</sup> Distinct differences in the diameter and height of the three polysaccharides were also observed. The diameter and height of PCP (0.0–30.0 nm) exceeded that of PKP (0.5–6.0 nm) and PSP (0.0–10.0 nm).

**3.1.3 Thermal properties of polysaccharides.** The TGA curves of the three polysaccharides were similar and presented three-step degradation patterns (Fig. S4†). The first mass loss occurred when the total water content was approximately 11.52% for PCP, 10.35% for PKP, and 10.31% for PSP. This is due to the dehydration of bound water in polysaccharides.<sup>14</sup> The second mass loss for PCP, PKP and PSP took place at thermal decomposition temperatures of 223.54 °C, 223.20 °C, and 217.09 °C, resulting in weight losses of 65.32%, 69.04%, and 68.88%, respectively, which resulted from the depolymerization of the polysaccharide structures. Finally, as the temperature increased, the polysaccharide weights did not change.

**3.1.4 Rheological properties of polysaccharides.** As displayed in Fig. 5A, PCP, PKP, and PSP solutions displayed both shear-thinning and Newtonian fluid behaviors, which rely on the shear rate. This indicated that the apparent viscosity of PCP (997.39, 110.69, 22.74, and 4.57 mPa s) was higher than that of PSP (423.30, 29.72, 3.44, and 0.44 mPa s) and PKP (179.25, 29.54, 2.81 and 0.35 mPa s) at 0.1, 1.0, 10, and 100 s<sup>-1</sup>. As the shear rate increased from 0.1 to 100 s<sup>-1</sup>, decreasing viscosity was observed in the three polysaccharides, suggesting the shear-thinning behavior of the polysaccharides.<sup>20</sup> The viscosity of the polysaccharides remained almost unchanged at the high shear rates of 100–1000 s<sup>-1</sup>, indicating the presence of near-Newtonian fluid behavior. It has been reported that sugar chains slowly disentangle as the shear rate increases, leading to a Newtonian plateau at a high shear rate.<sup>28,29</sup>

Polysaccharides as biopolymers exhibit both liquid viscous and solid elastic properties.<sup>30</sup>  $G'$  and  $G''$  respectively represent the elastic and viscous features of the given samples.  $G'$  values were significantly higher than  $G''$  values, indicating that dispersions display a stronger elastic gel network.<sup>20</sup> The modulus  $G'$  and  $G''$  values of all the samples increased with increasing frequency and the storage modulus  $G'$  values were higher than the loss modulus  $G''$  within the frequency region for PCP, PKP, and PSP (Fig. 5B). This indicated that the three *Polygonatum* polysaccharides exhibited typical viscoelastic behaviors that are characteristic of elastic materials.<sup>20,30</sup> PCP showed the highest  $G'$  and  $G''$  values, indicating high viscoelasticity.

### 3.2 *In vitro* antioxidant activities of polysaccharides

DPPH and ABTS are stable free radicals that are typically used to assess the free radical-scavenging capacities of antioxidants.<sup>22</sup> Hydroxyl radicals are reactive oxygen species with strong oxidation ability that can attack adjacent biomolecules and lead to

tissue damage or cell apoptosis.<sup>22</sup> Superoxide anion radicals are the continuous outcome of certain enzymes in biological systems and negatively affect cellular components.<sup>30</sup> The free radical-scavenging abilities of PCP, PKP, and PSP are displayed in Fig. 6A–D and show that the three polysaccharides all significantly exhibited DPPH, ABTS, hydroxyl, and superoxide anion radical-scavenging abilities in a dose-dependent manner in the concentration range of 0.1 to 5.0 mg mL<sup>-1</sup>. At all test concentrations, PCP had a higher DPPH radical scavenging ability ( $IC_{50}$ , 2.04 mg mL<sup>-1</sup>) than PSP ( $IC_{50}$ , 3.07 mg mL<sup>-1</sup>) and PKP ( $IC_{50}$ , 4.10 mg mL<sup>-1</sup>). At a concentration of 5.0 mg mL<sup>-1</sup>, the ABTS radical-scavenging abilities of PSP ( $IC_{50}$ , 0.68 mg mL<sup>-1</sup>), PCP ( $IC_{50}$ , 0.85 mg mL<sup>-1</sup>) and PKP ( $IC_{50}$ , 1.61 mg mL<sup>-1</sup>) were 89.65%, 85.75%, and 68.29%, respectively. This indicates that PSP had the strongest ABTS radical scavenging ability. The hydroxyl radical-scavenging abilities of the three samples at 5.0 mg mL<sup>-1</sup> reached 88.82% for PCP ( $IC_{50}$ , 0.84 mg mL<sup>-1</sup>), 77.18% for PSP ( $IC_{50}$ , 1.04 mg mL<sup>-1</sup>), and 72.75% for PKP ( $IC_{50}$ , 1.26 mg mL<sup>-1</sup>), suggesting that PCP had better scavenging activity for hydroxyl radicals. In addition, the  $IC_{50}$  of PKP, PCP, and PSP for superoxide scavenging were 2.25, 2.75, and 3.46 mg mL<sup>-1</sup>, respectively. PKP (72.71%) and PCP (72.17%) showed relatively stronger superoxide scavenging capabilities than PSP (60.16%).

Metal chelating activity and reducing power are important indicators for potential antioxidant activity. Fig. 6E and F demonstrate that the chelating capabilities and the reducing power of the three polysaccharides all increased as the concentration increased from 0.1 to 5.0 mg mL<sup>-1</sup>. At 5.0 mg mL<sup>-1</sup>, the chelating ability of PCP reached 40.67%, which was higher than the other polysaccharides. The reducing powers of PCP and PKP at 4.0 mg mL<sup>-1</sup> and 5.0 mg mL<sup>-1</sup> were stronger than that of PSP.

### 3.3 Promotion of polysaccharides on GLP-1 secretion *in vitro*

In the present work, the effects of three *Polygonatum* polysaccharides on the secretion of GLP-1 from NCI-H716 cells were

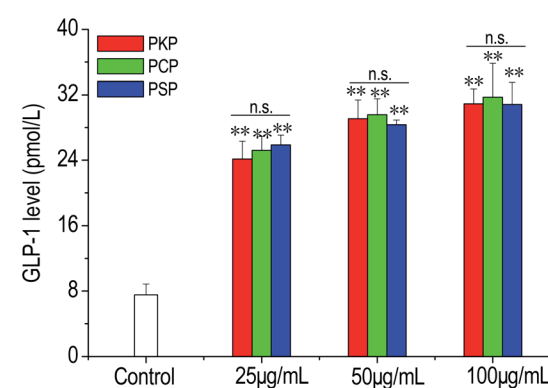
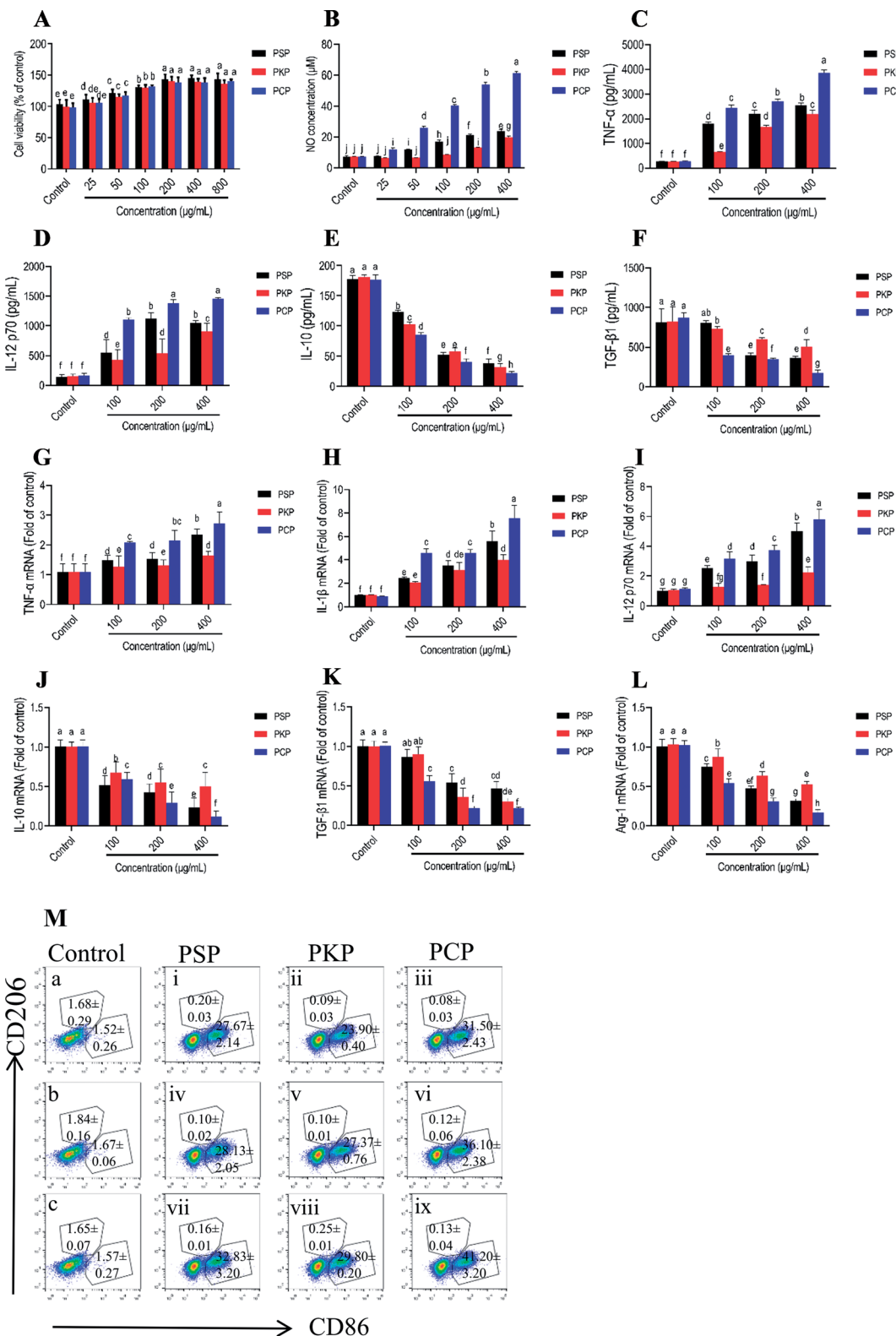


Fig. 7 GLP-1 levels in the supernatant of NCI-H716 cells after the stimulation of PKP, PCP, and PSP at the concentrations of 25–100 µg mL<sup>-1</sup>. The cells incubated in the medium without polysaccharides were used as the negative control. The data are presented as the mean  $\pm$  SD ( $n = 4$ ). \*\* indicates  $p < 0.01$  vs. control. n.s. indicates no significant difference between PKP, PCP, and PSP.





**Fig. 8** The effects of three *Polygonatum* polysaccharides on RAW264.7 cell viability (A), secretion levels of NO, TNF- $\alpha$ , IL-12, IL-10, and TGF- $\beta$  (B-F), and mRNA expression of IL-1 $\beta$ , TNF- $\alpha$ , IL-12, Arg-1, IL-10, and TGF- $\beta$  (G-L), and the cell surface expression of CD86 and CD206 in RAW264.7 cells (M) after treatment with 100 (Mi-iii), 200 (Miv-vi), and 400  $\mu\text{g mL}^{-1}$  (Mvii-ix) of PSP, PKP and PCP. The cells treated with medium without polysaccharide were used as the negative control (a-c). The values are presented as mean  $\pm$  SD ( $n = 4$ ). Different letters or letter combinations mean significant differences ( $p < 0.05$ ) in multiple-range analysis among the groups.

examined. The results demonstrated that compared to the control, PKP, PCP, and PSP significantly stimulated GLP-1 production from NCI-H716 cells in a dose-dependent manner (from 25 to 100  $\mu\text{g mL}^{-1}$ ) (Fig. 7). At all test concentrations, there was no significant difference in the stimulation of GLP-1 secretion between PSP, PKP, and PCP.

### 3.4 Regulation of polysaccharides on macrophage polarization *in vitro*

M1-polarized macrophages that are characterized by the elevated cell surface expression of CD86 release pro-inflammatory cytokines such as TNF- $\alpha$ , IL-1 $\beta$ , IL-12, and NO, to mediate the host defense against microbial infections and tumors, while alternatively activated M2 macrophages (which feature signature molecules such as CD206, IL-10, arginase-1 (Arg-1), and TGF- $\beta$ ) are involved in immune tolerance and tumor progression.<sup>31-33</sup> In this study, the potential effects of three *Polygonatum* polysaccharides on macrophage polarization were investigated by detecting symbolic signature molecules including NO, TNF- $\alpha$ , IL-12, IL-1 $\beta$ , IL-10, Arg-1 and TGF- $\beta$  protein or mRNA expression, as well as the cell surface expression of CD86 and CD206. As shown in Fig. 8A, none of the three polysaccharides were cytotoxic to RAW264.7 cells, and dose-dependently promoted cell proliferation at the concentration of 25–800  $\mu\text{g mL}^{-1}$ . The treatment with PCP at 25 to 400  $\mu\text{g mL}^{-1}$ , PKP at 200 to 400  $\mu\text{g mL}^{-1}$  and PSP at 50 to 400  $\mu\text{g mL}^{-1}$  could significantly promote the production of NO by the cells (Fig. 8B). Moreover, at the same test concentration, PCP had a greater promotive effect as compared to the other polysaccharides. In addition, the secretion levels of TNF- $\alpha$  and IL-12 were significantly increased, while levels of IL-10 and TGF- $\beta$  were obviously reduced in a dose-dependent manner after stimulation with PCP, PKP and PSP at 100 to 400  $\mu\text{g mL}^{-1}$  (Fig. 8C–F). The three polysaccharides (100 to 400  $\mu\text{g mL}^{-1}$ ) significantly up-regulated the mRNA levels of TNF- $\alpha$ , IL-12, and IL-1 $\beta$ , and down-regulated the mRNA levels of IL-10, TGF- $\beta$ , and Arg-1 (Fig. 8G–L). The expression of the M1 characteristic surface molecule CD86 was significantly elevated and M2 surface molecule CD206 expression (Fig. 8M) was markedly reduced after respective treatment with PCP, PKP and PSP at 100 to 400  $\mu\text{g mL}^{-1}$ .

## 4. Discussion

The rhizomes of *Polygonatum* are known as “Huangjing” in China and were recognized as the rhizomes from *P. cyrtponema*, *P. sibiricum*, and *P. kingianum* in Chinese Pharmacopoeia.<sup>1</sup> The total polysaccharides are considered as their component index, and most biological activities including anti-oxidative, immuno-regulation, and hypoglycemic effects of *Polygonati* rhizomes are related to polysaccharides.<sup>34</sup> So far, some *Polygonatum* polysaccharides have been reported, which include a gluco-fructan from *P. cyrtponema*,<sup>3,4</sup> galactomannan from *P. sibiricum*,<sup>5,6</sup> and glucomannan from *P. kingianum*.<sup>7,8</sup> However, most previous studies have focused on a single species. Further investigation and comparison of the physicochemical characteristics and

functional activities of polysaccharides from three *Polygonatum* rhizomes provided additional insight into using these three *Polygonatum* polysaccharides as functional agents.

In our study, we compared the physicochemical properties and biological activities related to free radical scavenging capacities, the promotion of GLP-1 secretion and the induction of macrophage polarization under uniform experimental conditions. Analysis of the monosaccharide composition revealed that PCP, PKP, and PSP contained fructose, glucose, galacturonic acid and galactose in different proportions. The same monosaccharide types suggested the homogeneity of the three polysaccharides but the difference in their content could be attributed to their different growing environments. Fructose accounts for a greater proportion in PCP, PKP, and PSP, which is consistent with previous studies.<sup>2-4</sup> Some polysaccharides containing a large amount of fructose have been demonstrated to have hypoglycemic effects through the promotion of GLP-1 secretion.<sup>10</sup> The molecular weight of the polysaccharide is a crucial factor in determining its bioactivity performance.<sup>35</sup> Our results indicated that the molecular weight of PCP was smaller than that of PKP or PSP. Generally, when compared to a polysaccharide with a larger molecular weight, a polysaccharide with lower molecular weight displays better biological activities because it can easily penetrate cell membranes.<sup>35</sup> FT-IR and NMR analysis demonstrated the presence of  $\beta$ -D-Fru,  $\alpha$ -D-Glcp, and  $\alpha$ -D-Galp sugar residues, and an O-acetyl group in PCP, PKP and PSP, suggesting that the three *Polygonatum* polysaccharides may be naturally acetylated fructans. It has been reported that the acetylated polysaccharides from *P. cyrtponema* and other natural plants exhibit stronger immuno-modulatory, and antioxidant activities.<sup>4</sup> The triple-helix structure is an important attribute allowing polysaccharides to perform their specific biological functions and has been proven by the connection between the triple-helix conformation of lentinan and its antitumor activity.<sup>17,24</sup> Therefore, the triple-helical structure of PKP, PSP, and PCP can impact the development of their specific bioactivities.

It has been suggested that polysaccharides with rheological properties can be used in food, biomedicine, and other industries.<sup>28</sup> Polysaccharide molecules containing polymer colloidal particles can attach to the huge chain molecules and hook and entangle them with each other, resulting in higher apparent viscosity and shear-thinning behavior.<sup>30</sup> PCP possessed the highest apparent viscosity of the three polysaccharides, revealing the stronger interactions among sugar chains and polymerization. The typical viscoelastic behavior of the three *Polygonatum* polysaccharides, particularly that of PCP, can allow them to be used as thickeners, texturizers and stabilizers in some solidified fermented food processing, such as the preparation of nutritional yoghurt. Furthermore, the shear-thinning properties of polysaccharides cause foods to become liquid, resulting in a thinner consistency.<sup>17</sup>

The biological activities of polysaccharides depend on their physicochemical properties.<sup>22</sup> It has been demonstrated that the antioxidant activities of plant polysaccharides are not influenced by a single factor, but rather a combination of factors. The radical scavenging ability of polysaccharides is



typically due to their electron- or hydrogen-donating abilities.<sup>14</sup> The carboxylic groups in polysaccharides can react with the hydrogen atom of the anomeric carbon. The high content of uronic acid in polysaccharides usually contributes to strong antioxidant activity.<sup>14,35,36</sup> The lower molecular weight of polysaccharides with more reductive hydroxyl groups results in stronger antioxidant activity.<sup>14,22,37</sup> It has also been reported that polysaccharides containing less glucose have better antioxidant abilities.<sup>14,38</sup> Therefore, PCP showed stronger antioxidant activity than PKP or PSP, which could be related to its lower molecular weight and glucose content. The relatively strong DPPH, ABTS and hydroxyl radical scavenging abilities of PSP could be responsible for the high amount of uronic acid found in PSP.

GLP-1 is an incretin hormone secreted from the intestinal endocrine L-cells in response to food nutrients.<sup>39</sup> Several studies have indicated that GLP-1 is a pleiotropic hormone that can perform multifaceted pharmacological functions including promoting insulin production from pancreatic  $\beta$ -cells, inhibiting glucagon secretion from pancreatic  $\alpha$ -cells, suppressing gastric emptying, decreasing food intake, reducing post-prandial blood glucose levels, and cardiovascular and neural protection.<sup>40,41</sup> Several studies have demonstrated that fructooligosaccharides can effectively enhance GLP-1 secretion by directly stimulating endocrine L-cells.<sup>42-44</sup> We previously reported that the *Polygonatum cyrtonema* polysaccharide can promote GLP-1 secretion and contains a large amount of fructose.<sup>10</sup> Similar effects of the three polysaccharides on the stimulation of GLP-1 secretion could be due to high amounts of fructose. Based on the multiple pharmacological properties of GLP-1, the promotion of GLP-1 secretion could be a way for *Polygonatum* polysaccharides to contribute to the management or prevention of diabetes. Therefore, these three *Polygonatum* polysaccharides can be used interchangeably to induce GLP-1 secretion and could be a valuable functional agent for treating hyperglycemia.

Macrophages are members of the innate immune system and play a central role in the innate host defense against external invaders and malignancies.<sup>32</sup> These cells have a highly heterogeneous cell population that exhibits remarkable plasticity and can undergo polarized activation in response to microenvironmental signals.<sup>33</sup> It was found that at the same test concentrations, PCP had the most potent effect on the induction of M1 polarization of macrophages by regulating signature molecules at protein and mRNA expression followed by PSP and PKP; there were significant differences between them, which might be due to their different physicochemical features including molecular weight, monosaccharide composition, tertiary structure, microstructure, thermal, and rheological properties. Recent studies have demonstrated that the modulation of macrophage polarization could represent a new method of treating certain diseases involving macrophage immunodeficiencies, such as obesity, cancer, and metabolic diseases.<sup>32,45-47</sup> Thus, *Polygonatum* polysaccharides can be used as dietary supplements but PCP, PKP, and PSP could not be applied interchangeably to regulate M1 macrophage polarization to treat macrophage immunodeficiency diseases.

The close relationship between the structure and bioactivity of plant polysaccharides has been extensively proven.<sup>23</sup> The distinct antioxidant activity and induction of M1 macrophages polarization effects of PCP, PKP, and PSP may depend on their specific polysaccharide structural characteristics, including the molecular size, molar ratio of monosaccharides, and glycosidic bond types. The precise structural characteristics responsible for the activities of *Polygonatum* polysaccharides still need to be further explored.

## 5. Conclusions

In this study, three polysaccharides (PCP, PKP, and PSP) were extracted from different *Polygonatum* plants. We identified major fructose and minor glucose, galacturonic acid, and galactose in different molar ratios in these polysaccharides. PCP, PKP and PSP had different uronic acid contents and molecular weights, as well as a triple-helical structure with similar functional groups and sugar residues. Differences in the microstructures of the three polysaccharides were also observed via SEM and AFM. PCP, PKP, and PSP all had similar thermal decomposition temperatures. All three polysaccharides have liquid viscosity properties, with PCP displaying the highest apparent viscosity. Furthermore, PCP exhibited obvious antioxidant activities, followed by PSP and PKP. They also potentially induced the M1 polarization of macrophages to different degrees. PCP had the most potent activity. However, there were no significant differences in the promotion of GLP-1 secretion in NCI-H716 cells. Our results indicate that PCP, PKP, and PSP can be used interchangeably to promote GLP-1 secretion, but not in antioxidant activity and the induction of M1 macrophage polarization. This indicates that it is necessary to identify the possible applications of the three *Polygonatum* polysaccharides and determine whether they can be used interchangeably. Overall, this study contributes to a better understanding of the relationship between the structure and bioactivity of *Polygonatum* polysaccharides.

## Conflicts of interest

The authors declared that they have no conflicts of interest to this work.

## Acknowledgements

This work was financially supported by National Key R&D Program of China (No. 2018 YFC1707004), National Natural Science Foundation of China (No. 32001694), Natural Science Foundation of Anhui Province of China (No. 2008085QH393), and University Natural Science Key Research Program of Anhui Province (No. KJ2020A0421).

## References

- 1 P. Zhao, C. Zhao, X. Li, Q. Gao, L. Huang, P. Xiao and W. Gao, The genus *Polygonatum* : a review of ethnopharmacology,



phytochemistry and pharmacology, *J. Ethnopharmacol.*, 2018, **214**, 274–291.

2 P. Zhao, X. Li, Y. Wang, L. Yan, L. Guo, L. Huang and W. Gao, Characterisation and saccharide mapping of polysaccharides from four common *Polygonatum* spp, *Carbohydr. Polym.*, 2020, **233**, 115836.

3 F. Liu, Y. Liu, Y. Meng, M. Yang and K. He, Structure of polysaccharide from *Polygonatum cyrtonema* Hua and the antiherpetic activity of its hydrolyzed fragments, *Antiviral Res.*, 2004, **63**(3), 183–189.

4 P. Zhao, H. Zhou, C. Zhao, X. Li, Y. Wang, Y. Wang, L. Huang and W. Gao, Purification, characterization and immunomodulatory activity of fructans from *Polygonatum odoratum* and *P. cyrtonema*, *Carbohydr. Polym.*, 2019, **214**, 44–52.

5 H. Zhang, Y. Cao, L. Chen, J. Wang, Q. Tian, N. Wang, Z. Liu, J. Li, N. Wang, P. Sun and L. Wang, A polysaccharide from *Polygonatum sibiricum* attenuates amyloid- $\beta$ -induced neurotoxicity in PC12 cells, *Carbohydr. Polym.*, 2015, **117**, 879–886.

6 K. Yelithao, U. Surayot, J. H. Lee and S. G. You, RAW264.7 cell activating glucomannans extracted from rhizome of *Polygonatum sibiricum*, *Prev. Nutr. Food Sci.*, 2016, **21**(3), 245–254.

7 H. Yan, J. Lu, Y. Wang, W. Gu, X. Yang and J. Yu, Intake of total saponins and polysaccharides from *Polygonatum kingianum* affects the gut microbiota in diabetic rats, *Phytomedicine*, 2017, **26**, 45–54.

8 W. Gu, Y. Wang, L. Zeng, J. Dong, Q. Bi, X. Yang, Y. Che, S. He and J. Yu, Polysaccharides from *Polygonatum kingianum* improve glucose and lipid metabolism in rats fed a high fat diet, *Biomed. Pharmacother.*, 2020, **125**, 109910.

9 L. Li, K. Thakur, B. Y. Liao, J. G. Zhang and Z. J. Wei, Antioxidant and antimicrobial potential of polysaccharides sequentially extracted from *Polygonatum cyrtonema* Hua, *Int. J. Biol. Macromol.*, 2018, **114**, 317–323.

10 S. Z. Xie, G. Yang, X. M. Jiang, D. Y. Qin, Q. M. Li, X. Q. Zha, L. H. Pan, C. S. Jin and J. P. Luo, *Polygonatum cyrtonema* Hua polysaccharide promotes GLP-1 secretion from enteroendocrine L-cells through sweet taste receptor-mediated cAMP signaling, *J. Agric. Food Chem.*, 2020, **68**, 6864–6872.

11 B. L. Somani, J. Khanade and R. Sinha, A modified anthrone-sulfuric acid method for the determination of fructose in the presence of certain proteins, *Anal. Biochem.*, 1987, **167**, 327–330.

12 M. Marion, A rapid and sensitive method for the quantitation of microgram quantities of protein utilizing the principle of protein-dye binding, *Anal. Biochem.*, 1976, **7**, 248–254.

13 N. Blumenkrantz and G. Asboe-Hansen, New method for quantitative determination of uronic acids, *Anal. Biochem.*, 1973, **54**(2), 484–489.

14 G. Chen, C. Li, S. Wang, X. Mei, H. Zhang and J. Kan, Characterization of physicochemical properties and antioxidant activity of polysaccharides from shoot residues of bamboo (*Chimonobambusa quadrangularis*): effect of drying procedures, *Food Chem.*, 2019, **292**, 281–293.

15 Y. Biao, H. Jian, C. Yao, C. Shu, H. De, D. Ju and C. Chong, Identification and characterization of antioxidant and immune-stimulatory polysaccharides in *flaxseed hull*, *Food Chem.*, 2020, **315**, 126266.

16 N. Li, C. Shi, S. Shi, H. Wang, J. Yan and S. Wang, An inulin-type fructan isolated from *Artemisia japonica* and its antiarthritic effects, *J. Funct. Foods*, 2017, **29**, 29–36.

17 Y. Chen, J. G. Zhang, H. J. Sun and Z. J. Wei, Pectin from *Abelmoschus esculentus*: optimization of extraction and rheological properties, *Int. J. Biol. Macromol.*, 2014, **70**, 498–505.

18 R. Zhu, X. Zhang, Y. Wang, L. Zhang, J. Zhao, G. Chen, J. Fan, Y. Jia, F. Yan and C. J. Ning, Characterization of polysaccharide fractions from fruit of *Actinidia arguta* and assessment of their antioxidant and antiglycated activities, *Carbohydr. Polym.*, 2019, **210**, 73–84.

19 W. Wei, L. Feng, W. R. Bao, D. L. Ma, C. H. Leung, S. P. Nie and Q. B. Han, Structure characterization and immunomodulating effects of polysaccharides isolated from *Dendrobium officinale*, *J. Agric. Food Chem.*, 2016, **64**(4), 881–889.

20 R. L. Zapata-Luna, T. Ayora-Talavera, N. Pacheco, E. García-Márquez, H. Espinosa-Andrews, A. Ku-González, J. Ruiz-Ruiz and J. C. Cuevas-Bernardino, Physicochemical, morpho-structural and rheological characterization of starches from three *Phaseolus* spp. landraces grown in Chiapas, *J. Food Meas. Charact.*, 2021, **15**, 1410–1421.

21 Y. Xu, G. Liu, Z. Yu, X. Song, X. Li, Y. Yang, L. Wang, L. Liu and J. Dai, Purification, characterization and antiglycation activity of a novel polysaccharide from black currant, *Food Chem.*, 2016, **199**, 694–701.

22 Y. Xu, X. Niu, N. Liu, Y. Gao, L. Wang, G. Xu, X. Li and Y. Yang, Characterization, antioxidant and hypoglycemic activities of degraded polysaccharides from blackcurrant (*Ribes nigrum* L.) fruits, *Food Chem.*, 2018, **243**, 26–35.

23 S. S. Ferreira, C. P. Passos, P. Madureira, M. Vilanova and M. A. Coimbra, Structure-function relationships of immunostimulatory polysaccharides: a review, *Carbohydr. Polym.*, 2015, **132**, 378–396.

24 R. Guo, L. Ai, N. Cao, J. Ma, Y. Wu, J. Wu and X. Sun, Physicochemical properties and structural characterization of a galactomannan from *Sophora alopecuroides* L. seeds, *Carbohydr. Polym.*, 2016, **140**, 451–460.

25 Z. Dou, C. Chen and X. Fu, The effect of ultrasound irradiation on the physicochemical properties and  $\alpha$ -glucosidase inhibitory effect of blackberry fruit polysaccharide, *Food Hydrocolloids*, 2019, **96**, 568–576.

26 J. Huo, J. Wu, M. Zhao, W. Sun, J. Sun, H. Li and M. Huang, Immunomodulatory activity of a novel polysaccharide extracted from Huangshui on THP-1 cells through NO production and increased IL-6 and TNF-alpha expression, *Food Chem.*, 2020, **330**, 127257.

27 K. Henriksen, S. Stipp, J. Young and M. J. Marsh, Biological control on calcite crystallization: AFM investigation of



coccolith polysaccharide function, *Am. Mineral.*, 2004, **89**(12), 1709–1716.

28 B. Wang, W. Zhang, X. Bai, C. Li and D. Xiang, Rheological and physicochemical properties of polysaccharides extracted from stems of *Dendrobium officinale*, *Food Hydrocolloids*, 2020, **103**, 105706.

29 H. Yang, J. Bai, C. Ma, L. Wang, X. Li, Y. Zhang, Y. Xu and Y. Yang, Degradation models, structure, rheological properties and protective effects on erythrocyte hemolysis of the polysaccharides from *Ribes nigrum* L, *Int. J. Biol. Macromol.*, 2020, **165**(Pt A), 738–746.

30 L. Li, B. Y. Liao, K. Thakur, J. G. Zhang and Z. J. Wei, The rheological behavior of polysaccharides sequential extracted from *Polygonatum cyrtonema* Hua, *Int. J. Biol. Macromol.*, 2018, **109**, 761–771.

31 R. T. Netea-Maier, J. W. A. Smit and M. G. Netea, Metabolic changes in tumor cells and tumor-associated macrophages: a mutual relationship, *Cancer Lett.*, 2018, **413**, 102–109.

32 D. G. DeNardo and B. Ruffell, Macrophages as regulators of tumour immunity and immunotherapy, *Nat. Rev. Immunol.*, 2019, **19**(6), 369–382.

33 Y. Feng, R. Mu, Z. Wang, P. Xing, J. Zhang, L. Dong and C. Wang, A toll-like receptor agonist mimicking microbial signal to generate tumor-suppressive macrophages, *Nat. Commun.*, 2019, **10**(1), 2272.

34 J. Zhang, H. Chen, L. Luo, Z. Zhou, Y. Wang, T. Gao, L. Yang, T. Peng and M. Wu, Structures of fructan and galactan from *Polygonatum cyrtonema* and their utilization by probiotic bacteria, *Carbohydr. Polym.*, 2021, **267**, 118219.

35 J. K. Yan, Y. B. Yu, C. Wang, W. D. Cai, L. X. Wu, Y. Yang and H. N. Zhang, Production, physicochemical characteristics, and *in vitro* biological activities of polysaccharides obtained from fresh bitter gourd (*Momordica charantia* L.) via room temperature extraction techniques, *Food Chem.*, 2021, **337**, 127798.

36 Z. B. Wang, J. J. Pei, H. L. Ma, P. F. Cai and J. K. Yan, Effect of extraction media on preliminary characterizations and antioxidant activities of *Phellinus linteus* polysaccharides, *Carbohydr. Polym.*, 2014, **109**, 49–55.

37 Z. Zhang, X. Wang, C. Liu and J. Li, The degradation, antioxidant and antimutagenic activity of the mucilage polysaccharide from *Dioscorea opposita*, *Carbohydr. Polym.*, 2016, **150**, 227–231.

38 H. Chen, X. Xu and Y. Zhu, Optimization of hydroxyl radical scavenging activity of exopolysaccharides from *Inonotus obliquus* in submerged fermentation using response surface methodology, *J. Microbiol. Biotechnol.*, 2010, **20**(4), 835–843.

39 A. Andersen, A. Lund, F. K. Knop and T. Vilsbøll, Glucagon-like peptide 1 in health and disease, *Nat. Rev. Endocrinol.*, 2018, **14**(7), 390–403.

40 T. D. Muller, B. Finan, S. R. Bloom, D. D'Alessio, D. J. Drucker, P. R. Flatt, A. Fritsche, F. Gribble, H. J. Grill, J. F. Habener, J. J. Holst, W. Langhans, J. J. Meier, M. A. Nauck, D. Perez-Tilve, A. Pocai, F. Reimann, D. A. Sandoval, T. W. Schwartz, R. J. Seeley, K. Stemmer, M. Tang-Christensen, S. C. Woods, R. D. DiMarchi and M. H. Tschop, Glucagon-like peptide 1 (GLP-1), *Mol. Metab.*, 2019, **30**, 72–130.

41 Y. Song, J. A. Koehler, L. L. Baggio, A. C. Powers, D. A. Sandoval and D. J. Drucker, Gut-proglucagon-derived peptides are essential for regulating glucose homeostasis in mice, *Cell Metab.*, 2019, **30**(5), 976–986.

42 N. M. Delzenne, P. D. Cani and A. M. Neyrinck, Modulation of glucagon-like peptide 1 and energy metabolism by inulin and oligofructose: experimental data, *J. Nutr.*, 2007, **137**(11), 2547S–2551S.

43 M. Kobori, S. Masumoto, Y. Akimoto and Y. J. Takahashi, Dietary quercetin alleviates diabetic symptoms and reduces streptozotocin-induced disturbance of hepatic gene expression in mice, *Mol. Nutr. Food Res.*, 2009, **53**(7), 859–868.

44 P. Phuwamongkolwiwat, T. Hira and H. Hara, A nondigestible saccharide, fructooligosaccharide, increases the promotive effect of a flavonoid, alpha-glucosylisoquercitrin, on glucagon-like peptide 1 (GLP-1) secretion in rat intestine and enteroendocrine cells, *Mol. Nutr. Food Res.*, 2014, **58**(7), 1581–1584.

45 Y. Tang, C. Govers, H. J. Wijchers and J. J. Mes, Macrophages treated with non-digestible polysaccharides reveal a transcriptionally unique phenotype, *J. Funct. Foods*, 2017, **36**, 280–289.

46 A. El-Kenawi, C. Gatenbee, M. Robertson-Tessi, R. Bravo, J. Dhillon, Y. Balagurunathan, A. Berglund, N. Vishvakarma, A. Ibrahim-Hashim, J. Choi, K. Luddy, R. Gatenby, S. Pilon-Thomas, A. Anderson, B. Ruffell and R. Gillies, Acidity promotes tumour progression by altering macrophage phenotype in prostate cancer, *Br. J. Cancer*, 2019, **121**(7), 556–566.

47 J. Ren, C. Hou, C. Shi, Z. Lin, W. Liao and E. Yuan, A polysaccharide isolated and purified from *Platycladus orientalis* (L.) Franco leaves, characterization, bioactivity and its regulation on macrophage polarization, *Carbohydr. Polym.*, 2019, **213**, 276–285.

